SOCIETY FOR EXPERIMENTAL BIOLOGY

Journal of Experimental Botany, Vol. 00, No. 0 pp. 1–17, 2026
https://doi.org/10.1093/jxb/erag061 Advance Access Publication 25 February 2026

RESEARCH PAPER

Pyriculol effects on plant defence in rice: a virulence-independent secondary metabolite enhances host immunity against *Magnaporthe oryzae*

Junning Ma[1], Jean-Benoît Morel[2], Michael Riemann[1], Stefan Jacob[3], and Peter Nick[1,*]

[1] Joseph Gottlieb Kölreuter Institute for Plant Sciences, Karlsruhe Institute of Technology, D-76131 Karlsruhe, Germany
[2] PHIM Plant Health Institute, Université de Montpellier, INRAE, CIRAD, Institut Agro, IRD, Montpellier, France
[3] Institut für Biotechnologie und Wirkstoff-Forschung gGmbH (IBWF), Kaiserslautern, Germany

* Correspondence: peter.nick@kit.edu

Received 3 November 2025; Accepted 30 January 2026

Editor: Wen-Ming Wang, Sichuan Agricultural University, China

Abstract

The fungal phytotoxin pyriculol, produced by *Magnaporthe oryzae*, is potentially implicated in rice blast pathogenesis due to its necrosis-inducing activity. However, its functional role remained enigmatic. Here, we demonstrate that pyriculol does not act as a virulence factor for *M. oryzae*, as pathogenicity assays using transgenic fungal strains with altered pyriculol biosynthesis showed no correlation between pyriculol levels and disease severity across diverse rice genotypes. Strikingly, exogenous application of pyriculol or its isomer pyriculariol significantly enhanced rice resistance to *M. oryzae*, reducing lesion expansion by 30% and amplifying oxidative burst and defence-related gene expression (*OsPR1a*, *OsPBZ1*, and *OsCPS4*). Mechanistically, pyriculol mimicked salicylic acid (SA) by suppressing early jasmonate (JA) biosynthesis genes (*OsAOS1/2* and *OsAOC*) and JA-responsive JAZ transcripts post-wounding, yet uniquely spared *OsJAR1*, enabling systemic JA-Ile conversion from methyl jasmonate. This selective modulation decoupled local JA–SA antagonism, promoting SA-driven defence priming while permitting systemic JA signalling. Histological analyses revealed that pyriculol-induced host cell death restricted fungal hyphal progression, synergizing with pathogen-triggered phytoalexin biosynthesis. Our findings redefine pyriculol as a fungal metabolite that paradoxically bolsters rice immunity via phytohormone crosstalk, offering novel insights into host–pathogen co-evolution and potential applications in plant defence potentiation.

Keywords: Jasmonate signalling, *Magnaporthe oryzae*, phytohormone crosstalk, pyriculol, rice blast resistance, salicylic acid.

Introduction

Rice (*Oryza sativa*) is one of the most crucial staple crops, feeding a significant portion of the global population. However, its production is threatened by various pathogens, with *Magnaporthe oryzae* (rice blast fungus) standing out as a devastating fungal pathogen, causing annual rice yield losses equivalent to feeding 60 million people (Yan *et al.*, 2023). This fungal pathogen exhibits a remarkable ability to infect rice plants and has become a primary focus of research due to its significant impact on global food security. In order to develop novel and effective disease management strategies, a thorough understanding of the mechanisms behind virulence of the pathogen as well as the mechanisms behind the immunity of the host is crucial.

Rice harbours defence mechanisms to overcome the pervasive threats posed by pathogens such as *M. oryzae*. In addition to structural barriers, a basal form of innate immunity leads to accumulation of phytoalexins. However, specific pathogen strains inject effectors able to suppress basal immunity. In response, some genotypes have evolved strain-specific forms of immunity triggered by these effectors (for a review, see Liu *et al.*, 2013). The regulation of these two layers of defence depends on phytohormones, with the isoleucine conjugate of jasmonic acid (JA) activating basal immunity, and salicylic acid (SA) inducing effector-triggered immunity (Duan *et al.*, 2014; Ma *et al.*, 2022). These pathways often interact, either in concert or antagonistically, to provide protection depending on the infection context.

The JA pathway is activated upon wounding (herbivory), but also in response to necrotrophic pathogens. These stress signals lead to cleavage of α-linolenic acid from membrane lipids by specific lipases in the plastid membrane, such that this polyunsaturated fatty acid becomes accessible to a lipoxygenase, initiating the oxylipin pathway (for a comprehensive review, see Wasternack and Feussner, 2018). The resulting JA is not bioactive, but needs to be ligated to isoleucine by a jasmonoyl-L-isoleucine synthase (OsJAR1) to generate the biologically active JA-Ile (Riemann *et al.*, 2013; Shimizu *et al.*, 2013). Alternatively, JA can be methylated, generating the volatile methyl jasmonate (MeJA) that can act as a systemic signal. In the recipient cell, MeJA is demethylated and then converted to JA-Ile (Seo *et al.*, 2001). No matter whether the bioactive JA-Ile has been generated locally or captured systemically, it will bind to the JASMONATE-ZIM-DOMAIN (JAZ) proteins that are complexed with the F-box protein CORONATINE INSENSITIVE 1 (OsCOI1) and, upon binding of the JA-Ile ligand, becomes proteolytically degraded (Wasternack and Feussner, 2018). As a result, the transcription factor gene *OsMYC2* is activated and leads to the expression of JA-responsive genes involved in defence, development, and stress tolerance (Uji *et al.*, 2016), such as those encoding the flavonoid phytoalexin sakuranetin (Riemann *et al.*, 2013), but also those encoding diterpenoids such as momilactones (Kato-Noguchi, 2023).

SA is a central player in the defence against biotrophic pathogens. In contrast to dicotyledonous plants, rice accumulates high levels of SA even without pathogen infection (Silverman *et al.*, 1995). However, most of this SA is glycosylated by the transferase OsSGT1, providing a back-up that can be readily mobilized in case of need (Umemura *et al.*, 2009). Also, SA will lead to the accumulation of phytoalexins, including diterpenoids, such as momilactones, mostly mediated by a transcriptional cascade centring around *OsWRKY45* (Akagi *et al.*, 2014).

The interaction between SA and JA signalling forms a critical nexus orchestrating the two levels of innate immunity against *M. oryzae*. In contrast to the canonical paradigm, where the two hormones act as antagonists (reviewed in Thaler *et al.*, 2012), they seem to act synergistically during the pathogen defence of rice (for a review, see Tamaoki *et al.*, 2013). For instance, several defence-related genes, such as *OsPBZ1*, *OsPR1a*, and *OsPR1b*, are induced by both hormones (Tamaoki *et al.*, 2013), which is also true for genes encoding key enzymes involved in the synthesis of the diterpenoid phytoalexin, such as *OsCPS2* and *OsCPS4* (Akagi *et al.*, 2014; Ma *et al.*, 2022). On the other hand, depending on the infection strategy of the pathogen (necrotrophic versus biotrophic), a transcriptional cascade launched by ETHYLENE-INSENSITIVE3-LIKE 3 decides between activation of either SA or JA biosynthesis and signalling (Zhu *et al.*, 2024). The difference might be in the timing, since this cascade is activated several hours later than the induction of the pathogenesis-related (PR) genes mentioned above. The down-regulation of SA from 1 d after application of JA to rice leaves (Tamaoki *et al.*, 2013) points in a similar direction. The antagonism between JA and SA in rice might, therefore, be interpreted as attenuating fine-tuning rather than as activation of defence.

Plant pathogens have evolved a multitude of strategies to subvert the defence mechanisms of their hosts, often employing effectors that manipulate phytohormone synthesis or signalling to facilitate infection. As central regulators of immunity, the JA and SA pathways are preferential targets for effectors. A well-known example is coronatine, produced by the bacterial biotrophic pathogen *Pseudomonas syringae*. It mimics JA and antagonizes SA, which is required for the hypersensitive response (HR) in the host *Arabidopsis thaliana*, thereby promoting disease development (Brooks *et al.*, 2005). Likewise, the stem rust fungus *Puccinia graminis* f. sp. *tritici* produces auxin by expressing a tryptophan 2-monooxygenase gene leading to the accumulation of the auxin precursor indole-3-acetamide, thereby facilitating its infection (Yin *et al.*, 2014). Along a similar line, the biotrophic fungal pathogen *Ustilago maydis* injects the enzyme chorismate mutase (Cmu1) into host cells, interfering with SA biosynthesis of the host and, thereby, inactivating a HR, such that there is no efficient strategy to contain the fungus (Djamei *et al.*, 2011).

In rice, *M. oryzae* produces a cytokinin-like effector that interferes with rice immunity, leading to islands of green tissues within the infected leaf, which allows the fungus to forage sugars and amino acids (Chanclud *et al.*, 2016). In this context, fungal secretion of two salicylaldehyde-mimicking polyketides, pyriculol and pyriculariol, is interesting (Iwasaki *et al.*, 1969; Kono *et al.*, 1991), since these compounds can induce either necrotic lesions or 'green island' symptoms on detached rice leaves, depending on the method of application (Suzuki *et al.*, 1986; Lokeshwari and Suryanarayanan, 1992). In our previous work unravelling the biosynthesis of these compounds (Jacob *et al.*, 2017), we identified *MoPKS19* as the essential polyketide synthase gene, observing that its transcript abundance correlates directly with pyriculol biosynthesis rates. Through the generation of a comprehensive set of mutants in

the *M. oryzae* 70-15 background, we dissected the regulation and product profiles of the pathway. Specifically, deletion of *MoPKS19* abolished the production of pyriculol, pyriculariol, and their dihydro derivatives. We further characterized a putative oxidase-encoding gene, *MoC19OX1*, adjacent to *MoPKS19*. Its deletion yielded a mutant producing exclusively dihydropyriculol and dihydropyriculariol, whereas overexpression of *MoC19OX1* resulted in a strain producing only pyriculol. Additionally, we identified two transcription factors within the cluster, MoC19tf1 and MoC19tf2, acting as negative regulators; strains ΔMoC19tf1 and ΔMoC19tf2 consequently exhibited hyperaccumulation of pyriculol. While extracts from the *MoPKS19* and *MoC19OX1* deletion mutants failed to induce lesions on rice leaves, confirming pyriculol and pyriculariol as the sole lesion-inducing metabolites under these conditions, the mutants themselves remained as pathogenic as the wild type (Jacob *et al.*, 2017). This finding poses a challenging question: why does the pathogen waste energy producing a lesion-inducing secondary metabolite if the phytotoxin is not strictly required for disease development?

In order to go beyond this first counter-intuitive result of an absence of a role in infection of such close derivatives of SA, we decided to further evaluate mutants in different contexts. Indeed, it might be crucial to consider more than one host genotype, since immunity-related cell death is embedded in a co-evolutionary context and often requires specific host alleles to become manifest (for a review, see Friesen *et al.*, 2008. Therefore, in the current study, a panel of both *indica* and *japonica* host genotypes were investigated with respect to their responses to a set of transgenic *M. oryzae* strains, where the accumulation of pyriculol was modulated. To gain insight into the role of phytohormonal status during infection, we used wounding as input to activate JA signalling, as well as exogenous SA and pyriculol to test the effect on the accumulation of transcripts related to JA synthesis and response, as well as of SA response. In parallel, we assessed the responses of a panel of defence genes (Ma *et al.*, 2022) and cellular defence responses to infection with *M. oryzae* in the absence or presence of pyriculol. We arrive at a novel hypothesis, where pyriculol might act as decoupler of local versus systemic defence responses.

Materials and methods

M. oryzae strains with modulated pyriculol accumulation

The study used the strain *M. oryzae* 70-15 along with six mutants generated in this strain, where the level of pyriculol was either elevated, reduced, or similar as compared with the wild type (Supplementary Table S1). These strains were previously characterized for their capacity to synthesize pyriculol and its derivatives (Jacob *et al.*, 2017). In strains ΔMoC19tf1 and ΔMoC19tf2, two cluster-specific transcription factor genes, *MoC19tf1* and *MoC19tf2*, respectively, had been deleted. Since both factors were found to act individually as negative regulators repressing expression of the central polyketide synthase gene *MoPKS19*, their deletion led to higher accumulation of pyriculol. In contrast, strain ΔMoPKS19, with a deleted gene encoding the essential polyketide synthase (*MoPKS19*), failed to accumulate any pyriculol, pyriculariol, or their dihydro derivatives. Similarly, strain ΔMoC19OX1, with a deleted putative oxidase gene (*MoC19OX1*), failed to accumulate any pyriculol, but instead exclusively produced the precursors dihydropyriculol and dihydropyriculariol. In contrast, strain ΔMoEF1::C19OX1, overexpressing the *MoC19OX1* oxidase gene, accumulated higher levels of pyriculol and produced no dihydro intermediates, while strain MoC19OX1/OX1, which had been deleted and re-complemented for this oxidase, showed pyriculol levels that were comparable with the wild type. For comparison, the virulent strain 70-15 (Jacob *et al.*, 2017; Ma *et al.*, 2022) was used in some experiments as positive control. Strains were cultivated and inoculated in a standardized manner as described in Ma *et al.* (2022).

Evaluating pathogenicity

Pathogenicity was monitored using a panel of eight rice varieties. This panel represented a gradient of resistance to *M. oryzae*. The four *indica* varieties Bala, IR64 (both strongly resistant), Kasalath, and Co39 (both partially resistant) were used along with the four *japonica* varieties Azuzena and Nipponbare (both partially resistant), and Maratelli and Sariceltik (fully susceptible) (Supplementary Fig. S1). The plants were raised to an age of 3 weeks, and then inoculated with 5×10^4 spores ml^{-1} as described previously (Ma *et al.*, 2022).

At 6 d post-infection, the fully expanded flag leaves were sampled for symptom quantification and gene expression analysis. Symptoms were assessed using a classification system discriminating six grades of severity (Fig. 1A). Here, class 1 represented the absence of any lesions; class 2 represented small-sized and solid necrotic lesions without any whitish part; class 3 medium-sized necrotic lesions with a tiny whitish core; class 4 medium-sized whitish lesions with a necrotic ring; class 5 large whitish lesions with a necrotic ring; and class 6 large whitish lesion without a necrotic ring. As readout for disease severity, a Disease Index (DI) was determined as $DI=\Sigma i\times P_i$, where i denotes the severity class i, and P_i represents the percentage of lesions belonging to this class i. Three biological replicates were performed for this analysis. In each replicate, we sampled the fourth leaf blade from a minimum of three rice plants to evaluate disease symptoms.

To assess the plant response to the pyriculol-related strains of *M. oryzae*, we measured the expression of *OsPR1a*, *OsPBZ1*, and *OsCPS4* as defence-related marker genes by real-time quantitative PCR (RT-qPCR) at day 2 after inoculation using primers as described in Supplementary Table S2. RT-qPCR experiments were performed using the ΔΔCt method (Livak and Schmittgen, 2001). The stability of two candidate reference genes, *OsGAPDH* (glyceraldehyde-3-phosphate dehydrogenase) and *OsU10* (ubiquitin 10), was evaluated across all experimental conditions and time points using both the geNorm (Vandesompele *et al.*, 2002) and NormFinder (Andersen *et al.*, 2004) algorithms. Both algorithms confirmed good stability for both reference genes across all conditions, with geNorm M values and NormFinder stability values consistently <0.5 (Supplementary Fig. S2). Gene expression data were normalized to the geometric mean of *OsGAPDH* and *OsU10*. Data represent means ±SD from three independent biological replicates, with each biological replicate analysed in technical triplicate.

Assessing the effect of pyriculol and salicylic acid on symptom expression in leaves

Caryopses of *O. sativa* ssp. *japonica* cv 'Nihonmasari' were pre-selected for uniformity and health, and then dehusked for surface sterilization. Subsequently, they were imbibed in 70% ethanol, and then were rinsed twice with sterilized water before being soaked in a 5% sodium hypochlorite solution and incubated on a shaker at 250 rpm for 20 min. The sterilized caryopses were then sown using flame-sterilized tweezers in Magenta boxes filled with 100 ml of autoclaved 0.4% phyto-agar on a

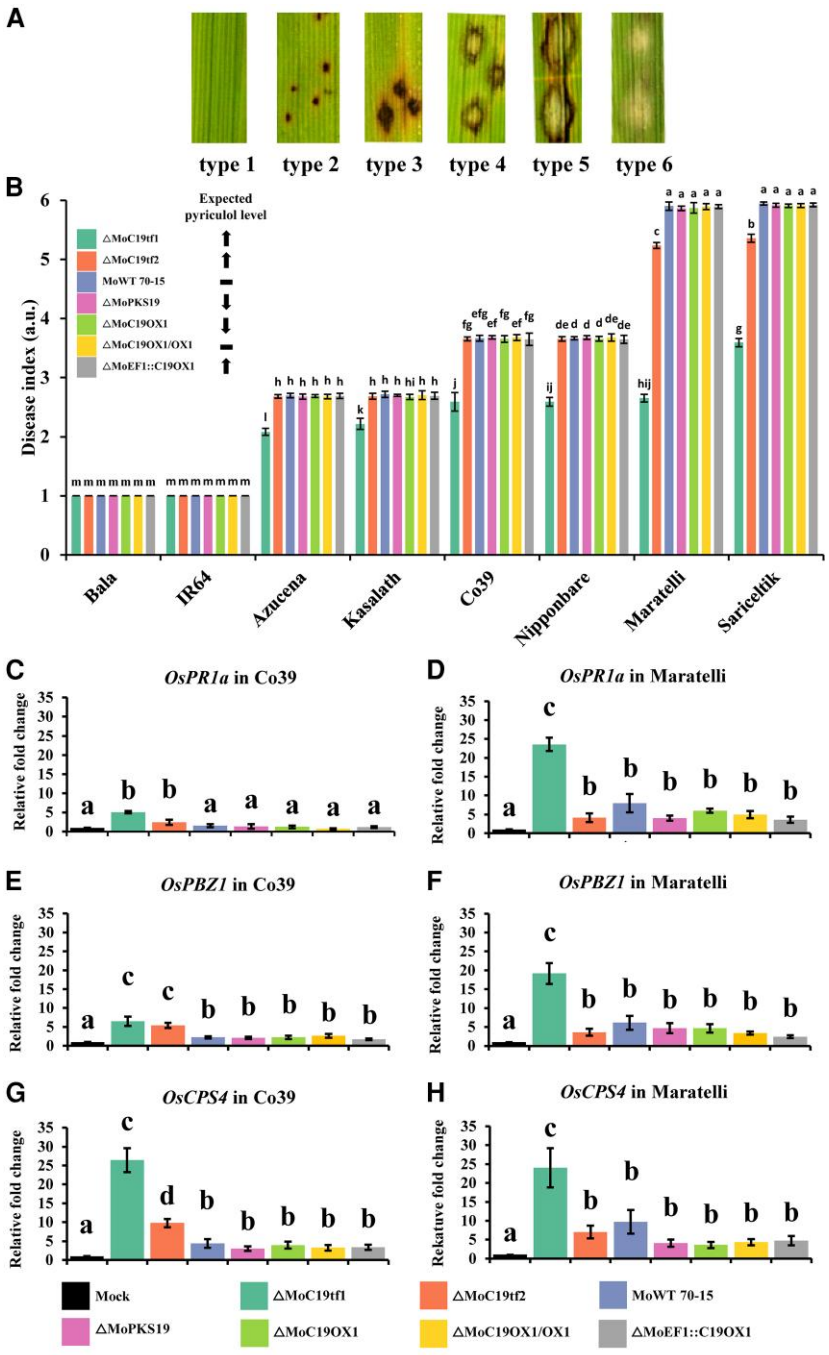

Fig. 1. Quantification of rice blast disease symptoms and defence-related gene expression in response to *M. oryzae* wild type and pyriculol-related transgenic strains. (A) Representative disease symptoms on rice leaves at 6 days post-inoculation (dpi), illustrating the six severity classes (Type 1–Type 6) used for disease assessment. Class 1, no lesions; Class 2, small, solid necrotic lesions; Class 3, medium-sized necrotic lesions with a small whitish center; Class 4, medium-sized whitish lesions with a necrotic ring; Class 5, large whitish lesions with a necrotic ring; and Class 6, large whitish lesions without a necrotic ring. (B) Disease index (DI) of eight rice varieties: Bala, IR64, Azucena, Kasalath, Co39, Nipponbare, Maratelli, and Sariceltik, after inoculation with seven *M. oryzae* strains: MoWT 70-15, Δ*MoC19tf1*, Δ*MoC19tf2*, Δ*MoPKS19*, Δ*MoC19OX1*, Δ*MoEF1::C19OX1*, and Δ*MoC19OX1*/OX1. DI was calculated as $\sum_i \times P_i$, where *i* is the severity class (1–6), and P_i is the percentage of lesions in class *i*. Three biological replicates were performed, each using a minimum of three plants. (C, E, G) Relative expression (using the ΔΔCt method) levels of defence-related genes *OsPR1a* (C), *OsPBZ1* (E), and *OsCPS4* (G) in the partially resistant rice variety Co39 at 48 h post-inoculation (hpi) with the seven *M. oryzae* strains, as determined by RT-qPCR. (D, F, H) Relative expression levels of defence-related genes *OsPR1a* (D), *OsPBZ1* (F), and *OsCPS4* (H) in the susceptible rice variety Maratelli at 48 hpi with the seven *M. oryzae* strains, as determined by RT- qPCR. Data represent mean values ±SE from three independent biological replicates. Different lowercase letters indicate statistically significant differences among treatments within each panel (P<0.05, Fisher's LSD test following one-way ANOVA).

UV-irradiated clean bench. The Magenta boxes were then placed in a plant growth chamber (CLF Plant Climatics, Wertingen, Germany) for 7 d with 12 h of light followed by 12 h of darkness, both at 28 °C. After 7 d, the rice seedlings were transplanted into a hydroponic culture system consisting of a glass bottle containing liquid medium (0.35 g l^{-1} Murashige and Skoog medium) and a floating polystyrene carrier where they were fixed. The rice plants were raised in the chamber for a further week, such that the experiment was initiated when they were 3 weeks old. Then, the blade of the uppermost fully expanded leaf was carefully sampled and cut into segments of ~3 cm width. Droplets of pyriculol (0, 0.16, 0.32, 0.64, 0.8, 1.6, and 6.4 mM), and SA (0, 0.2, 1, 2, 4, and 10 mM), both in 0.5% w/v gelatine as adhesive carrier, were placed on the leaf surface, and the segments were then allowed to develop symptoms in a Petri dish sealed with Nescofilm and incubated for an additional 2 d, under the same conditions in which plants had been grown before sampling. For evaluation, the leaves were digitally imaged, and the lesion areas determined from these images using the area tool of ImageJ (https://imagej.net/ij). For each treatment, three leaves from three independent biological replicates were scored for symptoms.

Assessing the effect of pyriculol and salicylic acid on wound-induced gene expression

Seedlings were foliar-sprayed until runoff with 0.8 mM pyriculol or SA, each dissolved in a 0.5% (w/v) gelatine solution. A control group was treated with 0.5% (w/v) gelatine alone. At 0.5 h post-treatment, the uppermost fully expanded leaf blade of each plant was wounded. Plants were exposed to wounding in a standardized manner when they were 3 weeks old (cultivation was exactly as described above). Seven cuts of 0.5 cm each were made by scissors in the transverse direction to the uppermost fully expanded leaf blade, at equal distances along the leaf blade. It should be noted that the wounded leaves were not excised but remained on the plant. The wounded leaves were then sampled at 0.5 h and 1 h after wounding treatment and immediately shock-frozen in liquid nitrogen. RNA was extracted and cDNA was synthesized as described in Ma *et al.* (2022), and the steady-state transcript levels for genes involved in JA biosynthesis (*OsAOS1*, *OsAOS2*, *OsAOC*, and *OsJAR1*), JA signalling (*OsJAZ8*, *OsJAZ9*, *OsJAZ10*, *OsJAZ11*, and *OsJAZ13*), and SA response (*OsSGT1* and *OsWRKY45*) were measured by RT-qPCR using the primers detailed in Supplementary Table S2. Gene expression data were normalized to the geometric mean of the validated reference genes *OsGAPDH* and *OsU10* (reference gene validation described above; Supplementary Fig. S2). Data represent means ±SD from three independent biological replicates, with each biological replicate analysed in technical triplicates.

Effect of pyriculol and pyriculariol on rice defence against *M. oryzae*

To assess the inhibitory effects of pyriculol and pyriculariol on *M. oryzae* spore germination, conidial suspensions of the *M. oryzae* strain Guy11 (5×10^4 spores ml^{-1}) were co-inoculated with varying concentrations of pyriculol (0–160 μM) or pyriculariol (0–640 μM) on sterile glass slides. The slides were incubated in the dark at 26 °C for 12 h to allow germination. Following incubation, spore germination was examined microscopically to determine compound-mediated inhibition. To ensure that downstream plant infection assays were not confounded by spore germination inhibition, a non-inhibitory concentration of each compound (160 μM) was selected for *in planta* studies. Three-week-old *O. sativa* cv Nihonmasari seedlings were spray-inoculated with the conidial suspension (5×10^4 spores m^{-1}) supplemented with either pyriculol or pyriculariol at 160 μM. Inoculation was performed as previously described (Ma *et al.*, 2022). After inoculation, plants were maintained in a dark dew chamber at 26 °C for at least 16 h to promote appressorium formation and initial infection. Subsequently, plants were transferred to a controlled-growth chamber for disease development. A solvent control (1% methanol in water) corresponding to the maximal methanol concentration used in the compound treatments was included in all assays to exclude vehicle effects.

The response to the inoculation was allowed to unfold over 6 d, when symptoms were assessed as outlined in 'Evaluating pathogenicity'. Additionally, a histological analysis was conducted with the objective of evaluating the presence of fungal growth in rice leaves, following a previously established protocol (Ma *et al.*, 2022). In parallel, 3,3'-diaminobenzidine (DAB) was utilized to visualize the production of H_2O_2 resulting from *M. oryzae* infection. Infected leaves were infiltrated in 1 mg ml^{-1} DAB at 4 °C over 2 d, and then cut into 3 cm segments for fixation in 75% (v/v) ethanol, 25% (v/v) chloroform, and 0.15% (v/v) acetic acid for an additional 2 d to enable the complete removal of chlorophyll. The degree of browning in this de-pigmented tissue can then be used to assess the degree of oxidative burst. The result was assessed by bright-field microscopy (ZEISS Axioscope at ×20 magnification), classifying the samples in four categories: (i) presence of an appressorium and a germ tube, but no oxidative burst of the host tissue; (ii) presence of an appressorium and a germ tube with oxidative burst only in the infected cell itself; (iii) presence of an appressorium and a germ tube with oxidative burst in multiple cells around the infection site; and (iv) progression of fungal development until the formation of invasive hyphae with oxidative burst in the host tissue. The fourth leaf blade from at least three rice plants was employed for the histological analysis, on which we counted 100 infection events for the classification.

Data analysis

Differences between samples were pairwise tested for statistical significance by a Student's *t*-test in Excel 2016. For multiple comparisons, we utilized a one-way ANOVA followed by Fisher's LSD test, with the aid of the R package Agricolae.

Results

We utilized a set of *M. oryzae* mutants previously engineered to exhibit distinct pyriculol profiles (Jacob *et al.*, 2017). This panel includes strains with abolished production (via deletion of the synthase MoPKS19 or oxidase MoC19OX1) and strains with hyperaccumulation (via deletion of negative regulators MoC19tf1/2 or oxidase overexpression). A key finding from the initial study was that pyriculol-deficient mutants remained virulent on rice cultivar Co39, despite the inherent phytotoxicity of the compound. This raised a paradox regarding the energy cost of its biosynthesis (Jacob *et al.*, 2017). To address whether this dispensability is general or host specific, we expanded the virulence analysis to a wider range of host genotypes.

Overaccumulation of pyriculol impacts *M. oryzae* pathogenicity

To test how pyriculol relates to virulence of *M. oryzae*, we mapped the pathogenicity of seven strains of *M. oryzae* where the accumulation of pyriculol was engineered to be either promoted or suppressed (for details, see the Materials and methods). This panel of strains was tested on a panel of rice varieties differing with respect to their resistance against the rice blast fungus. The symptoms were classified for severity (Fig. 1A), and the amplitude of disease symptoms was

quantified using the DI. The comparison of DI values (Fig. 1B) confirmed significant differences of the tested rice varieties in terms of resistance. Here, Bala and IR64 did not exhibit symptoms, followed by Azucena and Kasalath with mild symptoms. More severe symptoms were seen in Co39 and Nipponbare, and Maratelli and Sariceltik displayed maximal susceptibility.

When the individual *M. oryzae* strains were compared, five of them behaved identically, although their pyriculol levels should differ significantly. These five strains were all affected in biosynthetic enzymes. For instance, deletion of the polyketide synthase 19 (strain ΔMoPKS19) or the oxidase (ΔMoC19OX1) was expected to lead to a lack any pyriculol, while strain ΔMoEF1::C19OX1 should overexpress the oxidase and thus accumulate higher levels of pyriculol, and strain MoC19OX1/OX1, which had been deleted and re-complemented for this oxidase, should produce pyriculol levels comparable with the wild type and served as control. If pyriculol was a virulence factor, one would predict that the two strains carrying a deletion for the two biosynthetic enzymes should display significant decreases of symptom expression. Conversely, the strain overexpressing the oxidase should generate more severe symptoms. None of these implications has been observed. The disease scores were exactly the same as in strain MoC19OX1/OX1, representing the control.

A different pattern was seen when the transcription factors repressing pyriculol biosynthetic genes were deleted. For strain ΔMoC19tf1, in particular, symptoms were significantly suppressed, and to a weaker extent also for strain ΔMoC19tf2. Here, the implication was that removal of suppression should lead to higher levels of pyriculol, such that symptoms would be promoted. Again, the empirical test contradicted the implication. In fact, the experimental result was even the inverse of the prediction.

Thus, the levels of pyriculol established through engineering biosynthetic enzymes or regulators thereof did not show any correlation with the expression of symptoms, irrespective of the host genotype. This leads to the conclusion that pyriculol cannot be a virulence factor of *M. oryzae*.

To assess whether pyriculol might act as effector, the response of a panel of defence genes was investigated in two hosts differing with respect to their susceptibility. To be able to compare pathogenicity, the most resistant varieties (Bala and IR64) were not suitable because, here, the strong resistance would mask any difference between strains. We therefore selected Co39 as a host with intermediate susceptibility and Maratelli as a host with strong susceptibility for *M. oryzae* for this analysis. As readout, we selected the transcript for the acidic PR protein OsPR1a (Mitsuhara *et al.*, 2008) and the PR10a protein OsPBZ1, an RNase (Rakwal *et al.*, 2001), in addition, OsCPS4, a key enzyme for diterpene labdane phytoalexins, was probed (Lu *et al.*, 2018). Steady-state transcript levels were measured at day 2 after inoculation. Irrespective of gene and transcript, the highest expression was induced by strain ΔMoC19tf1, where the inactivation of the repressor is expected to accumulate higher levels of pyriculol (Fig. 1C–H). Transcript levels in the other strains were negligible in comparison. On the background of this general pattern, the induction pattern exhibited a salient difference: while the two host genotypes produced the same induction for the phytoalexin synthesis transcript *OsCPS4* (Fig. 1G, H), the two PR genes were only weakly induced in the more resistant Co39, but ∼5-fold more in the susceptible Maratelli (Fig. 1C–F). However, a closer look showed that, for *OsPR1a*, the ground levels in Co39 were higher than in Maratelli (Supplementary Fig. S3A, B), such that Co39, despite a lower induction factor, reached the same steady-state level for this transcript as seen in Maratelli. For *OsPBZ1*, the steady-state ground level in Co39 was significantly higher than in Maratelli, but the induction in Maratelli was much more pronounced as compared with Co39.

Overall, the deletion mutant ΔMoC19tf1 was not only the most avirulent strain, reflected by the smallest DI value, but also the strain with the strongest ability to induce the three tested defence-related genes. The expression of PR genes was higher in the susceptible rice variety Maratelli as compared with the more resistant Co39. Thus, the induction of PR genes correlates with symptom expression. On the other hand, the strain expected to show the highest level of pyriculol, because a negative regulator is deleted, is the strain evoking the strongest response of defence genes. If pyriculol acted as an effector, the opposite would be expected.

Pyriculol and salicylic acid induce lesion expansion in a concentration-dependent manner

To obtain insight into the potential role of pyriculol during infection by *Magnaporthe*, we investigated the leaf response to rising concentrations of pyriculol alone, without the presence of the fungus. Since pyriculol strongly resembles SA, we also recorded a dose–response relationship for SA.

Rice leaf segments treated with either pyriculol or SA developed extensive lesions around the application site. These lesions were characterized by a whitish core surrounded by a blackish necrotic ring (Fig. 2A). For both pyriculol and SA, we observed a dose-dependent expansion of lesion size. While this dose dependence was comparable (Fig. 2B), pyriculol seemed to be somewhat more effective than SA. To reach a lesion size of 0.03 cm^2, ∼2 mM pyriculol was needed, while SA induced this area earliest at ∼6 mM. Even an SA concentration as high as 10 mM produced a necrotic area of 0.004 cm^2, while 6.4 mM pyriculol induced a 5-fold more extended necrotic area. We noted that while both compounds induce similar necrotic effects, the necrotic ring was more prominent in pyriculol-treated leaves, possibly due to the deposition of condensed phenolic compounds prior to cell death. This suggests that while pyriculol may act through the SA pathway, direct SA application might bypass the accumulation of these pigmented intermediates to initiate necrosis directly. Taken

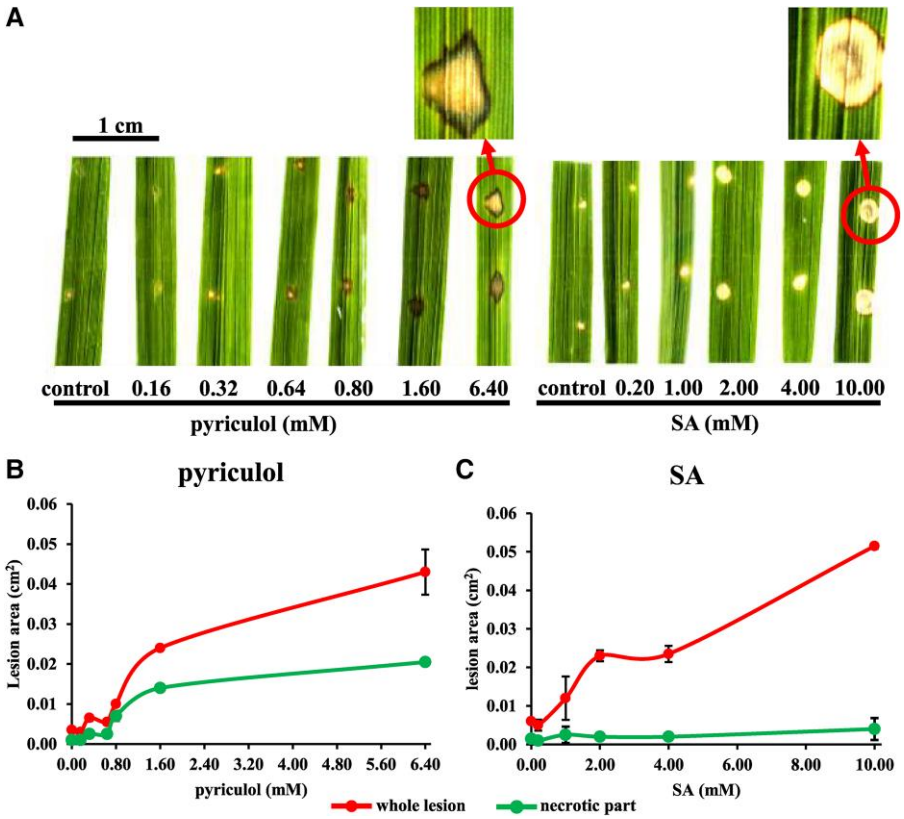

Fig. 2. Pyriculol and salicylic acid induce dose-dependent lesion formation on detached rice leaves. (A) Representative images of detached leaves of *O. sativa* cv Nihonmasari 2 d after treatment with increasing concentrations of pyriculol (0, 0.16, 0.32, 0.64, 0.80, 1.6, and 6.4 mM) or salicylic acid (SA; 0.2, 1.0, 2.0, 4.0, and 10.0 mM) in 0.5% (w/v) gelatine. (B) Quantification of lesion area from (A). Data represent means ±SE (n=3).

together, pyriculol can induce necrosis in a manner similar to SA, but more efficiently.

Pyriculol mimics salicylic acid with respect to early jasmonic acid biosynthesis genes, but not to JAR1

SA can repress JA responses, which is accompanied by inhibition of JA biosynthesis genes. Since pyriculol is structurally related to SA, we asked whether pyriculol modulates the responses of JA biosynthesis genes. To activate those genes, we used wounding as the trigger, following pre-treatment with either SA or pyriculol.

In the absence of wounding, both SA and pyriculol down-modulated the steady-state levels of *OsAOS1* (Fig. 3A), *OsAOS2* (Fig. 3B), *OsAOC* (Fig. 3C), and *OsOPR7* (Fig. 3D) to ~25–50% of the control. For *OsJAR1*, encoding the enzyme conjugating isoleucine to JA, the responses differed. Here, SA did not cause a change, while pyriculol repressed this gene significantly to around half of the control level (Fig. 3E). Wounding induced the expression of all genes, most pronounced for *OsAOS2* (Fig. 3B), where transcripts were induced by an order of magnitude, while the amplitudes of *OsAOC* (Fig. 3C) and *OsJAR1* (Fig. 3D) were the lowest (~3-fold). This induction was significantly mitigated by SA and pyriculol for *OsAOS1*, *OsAOS2*, *OsAOC*, and *OsOPR7* in a comparable manner (Fig. 3A–D). For OsAOC, this mitigation was transient and faded away after 30 min (Fig. 3C). Again, the situation for *OsJAR1* differed (Fig. 3E). Here, SA did not inhibit the induction by wounding, while pyriculol did—this difference remained transient however, and was only seen for 30 min.

In summary, pyriculol mimicked the effect of SA for the early JA biosynthesis genes (*OsAOS1*, *OsAOS2*, *OsAOC*, and *OsOPR7*), but not for *OsJAR1*, encoding the enzyme catalysing the final step leading to the bioactive conjugate JA-Ile.

Pyriculol mimics salicylic acid with respect to wound-induced gene expression

The bioactive signal, the isoleucine conjugate of JA (JA-Ile), triggers the degradation of JAZ proteins, culminating in the de-repression of JA-responsive genes. Among those targets are also the *JAZ* genes themselves, such that their induction can be used as a proxy for the presence of JA-Ile. Expression of *OsJAZ8*, *OsJAZ9*, *OsJAZ10*, *OsJAZ11*, and *OsJAZ13*, in particular, is tightly linked to the presence of JA-Ile (Ma *et al.*, 2022), and these genes are therefore expected to be up-regulated by wounding. Thus, antagonistic effects of SA and pyriculol on

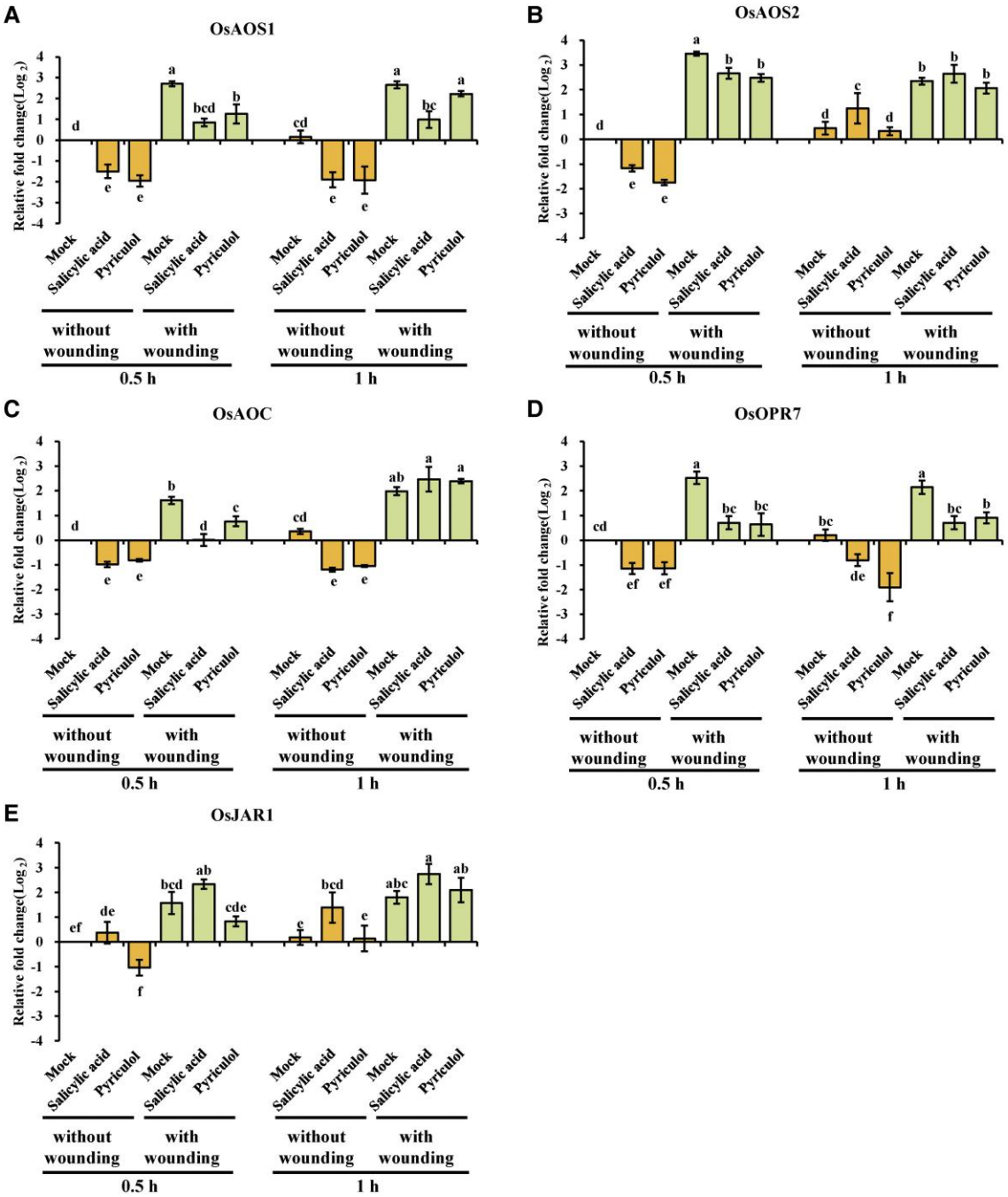

Fig. 3. Pyriculol and salicylic acid differentially modulate wound-induced expression of jasmonate biosynthesis genes in rice. Relative transcript abundance of (A) *OsAOS1*, (B) *OsAOS2*, (C) *OsAOC*, (D) *OsOPR7*, and (E) *OsJAR1* in leaves of 3-week-old rice seedlings. Plants were pre-treated via foliar spray with 0.5% (w/v) gelatine (Mock), 0.8 mM pyriculol, or 0.8 mM salicylic acid (SA), each dissolved in 0.5% gelatine. After 0.5 h, the uppermost fully expanded leaves were mechanically wounded (seven transverse cuts). Wounded leaves were sampled at 0.5 h and 1 h (H) post-wounding. Gene expression was determined by RT-qPCR, normalized to *OsG3PDH* and *Ubiquitin 10* reference genes using the $2^{-\Delta\Delta Ct}$ method. Data represent mean values ±SE from three independent biological replicates. Orange bars indicate unwounded samples; green bars indicate wounded samples. Different letters above bars denote statistically significant differences within each time point and treatment group ($P<0.05$, Fisher's LSD test following ANOVA).

JA responses should become manifest as a reduced induction of these genes by wounding.

In fact, all of these *JAZ* genes are clearly rapidly, but transiently, induced by wounding (Fig. 4A–E)—the inducibility ranges from ~5-fold (*OsJAZ8*, Fig. 4A) to >200-fold (*OsJAZ13*, Fig. 4E) within 30 min. Later, the steady-state levels decline again, especially for *OsJAZ10* (Fig. 4C) and *OsJAZ13* (Fig. 4E), where the values at 60 min have dropped

by ~8 times as compared with the values seen at 30 min. For the other *JAZ* genes, the decline is slower. With the exception of *OsJAZ10* (Fig. 4C), pre-treatment with SA alone causes a slight but significant repression (~2- to 4-fold, depending on the gene), which persists in the case of *OsJAZ8* (Fig. 4A) and *OsJAZ9* (Fig. 4B), but remains transient for the remaining three genes (Fig. 4C–E) and is followed at 60 min by a slight induction of a similar amplitude. Pyriculol strictly follows the same pattern, but mostly at a lower amplitude. In combination with wounding, SA significantly dampens the induction in the case of *OsJAZ8* (Fig. 4A), *OsJAZ9* (Fig. 4B), *OsJAZ11* (Fig. 4D), and *OsJAZ13* (Fig. 4E). This effect remains mostly transient, however, and disappears within 1 h. The only gene for which SA cannot dampen the induction by wounding is *OsJAZ10* (Fig. 4C). Again, pyriculol mimics the effect of SA almost perfectly, even with respect to the deviating pattern for *OsJAZ10* (Fig. 4C). The only case where it deviates significantly is the persistent inhibition of *OsJAZ9* (Fig. 4B). Here, the partial mitigation of the wounding effect has already faded away at 60 min, while it still persists for SA.

Overall, SA mitigates the response of *JAZ* genes to wounding, and pyriculol mimics this mitigating activity even with respect to small details.

The expression patterns of *OsSGT1* and *OsWRKY45*, used as reporters for SA responses, were rapidly and persistently induced by wounding, with both genes also activated by SA and, to a lesser extent, pyriculol (Fig. 4F, G). While pyriculol treatment enhanced the response of *OsWRKY45* under wounding conditions, SA did not show such an effect. Similarly, *OsSGT1* expression was induced by both SA and pyriculol, with a further increase upon wounding. Hierarchical clustering of representative JA signalling and SA-responsive genes (Fig. 4H) revealed that pyriculol-treated samples clustered closely with SA-treated samples, indicating similar regulatory effects on defence-related genes. Wound-induced activation of JAZ genes, including *OsJAZ9*, *OsJAZ10*, *OsJAZ11*, and *OsJAZ13*, was attenuated by both SA and pyriculol to varying degrees, suggesting differential suppression across the JAZ family. Conversely, SA-dependent genes such as *OsSGT1* and *OsWRKY45* were strongly induced by both SA and pyriculol, with enhanced expression under combined wounding and hormonal treatments. These findings suggest that pyriculol mimics SA in modulating JA signalling and activating SA-responsive pathways, reinforcing the idea of a complex interaction between the two signalling networks.

Pyriculol and pyriculariol improve resistance of Nihonmasari to *M. oryzae*

To investigate whether pyriculol or pyriculariol modulates host susceptibility to *M. oryzae*, we applied each compound at non-inhibitory concentrations (as established in Supplementary Fig. S4) during leaf inoculation with the virulent *M. oryzae* strain Guy11. Both compounds significantly reduced lesion development even at 40 μM, with a more pronounced suppression observed at 160 μM (Fig. 5A). Quantitative analysis of disease severity revealed an ~25% reduction in symptom area at 40 μM and up to 33% at 160 μM for both compounds (Fig. 5B).

To rule out the possibility that this mitigation effect was due to impaired spore viability or germination, we independently assessed conidial germination across a range of concentrations (Supplementary Fig. S4A). No detectable inhibition of germination was observed for either compound at concentrations up to 160 μM. Germination of *M. oryzae* spores was only moderately affected at 320 μM pyriculariol, with germination rates reduced by ~50%, and was fully suppressed only at 640 μM. Thus, the reduction in disease symptoms observed *in planta* is unlikely to result from direct antifungal activity at the applied concentrations, but rather suggests a potential modulation of host responses or pathogen virulence.

Together, these results demonstrate that the reduction in disease symptoms is not attributable to a direct suppression of spore germination. Instead, the effective concentrations that conferred symptom mitigation were well below the threshold required to inhibit fungal development at early stages. This suggests that pyriculol and pyriculariol act either by interfering with later stages of pathogen infection or by modulating host immune responses that restrict fungal colonization and symptom progression.

Pyriculol amplifies cell death and oxidative burst upon infection

To understand how pyriculol mitigated the symptoms caused by *M. oryzae*, we assessed defence responses on the histological level, staining simultaneously for fungal hyphae and peroxide accumulation as readout for oxidative burst. The results were classified into four types of events (Fig. 6A): formation of the appressorium and germ tube without any host cell death; with host cell death confined to the infected cell itself; with host cell death extending into the adjacent cells; and formation of invasive hyphae without any host cell death. We observed that pyriculol significantly reduced the frequency of events without host cell death, while the frequency of cell death, both localized and systemic, was increased by ~50% of the values seen in the control. The accumulation of hydrogen peroxide (H_2O_2), monitoring oxidative burst, was graded into three classes (Fig. 6C), either absence of H_2O_2 around the infection site, localized accumulation of H_2O_2 in the infected cell, or systemic accumulation extending to the adjacent cells. Here, we observed that pyriculol significantly (by ~20%) reduced the frequency of infection events without oxidative burst, while systemic oxidative burst was increased from 4.5% to 18.6%, corresponding to a 4-fold increase. The frequency of cells with localized oxidative burst was unchanged at ~20%. This means that around the same proportion of cells had changed from localized to systemic oxidative burst as cells had changed from the absence of oxidative burst to localized oxidative burst.

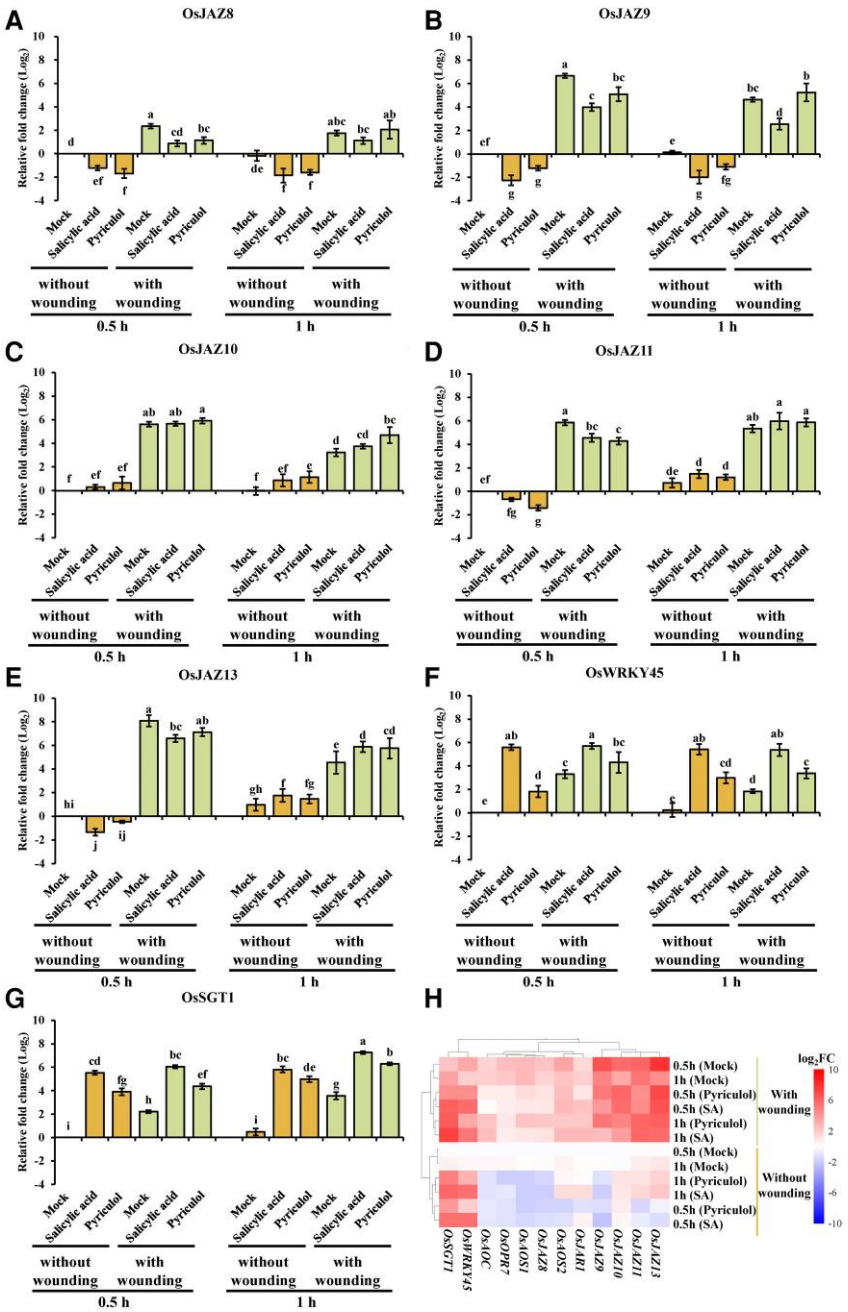

Fig. 4. Pyriculol and salicylic acid (SA) differentially modulate wound-induced expression of jasmonate (JA)- and SA pathway-related genes in rice. (A–G) Relative transcript levels of selected JA signalling repressors (A) *OsJAZ8*, (B) *OsJAZ9*, (C) *OsJAZ10*, (D) *OsJAZ11*, and (E) *OsJAZ13*, and the SA-responsive marker genes (F) *OsSGT1* and (G) *OsWRKY45* determined by RT-qPCR. Three-week-old rice seedlings (cv Nihonmasari) were foliar-sprayed with mock solution (0.5% w/v gelatine), 0.8 mM pyriculol, or 0.8 mM SA (both dissolved in mock solution). After 0.5 h, the uppermost fully expanded leaves were either left unwounded (orange bars) or mechanically wounded (seven 0.5 cm transverse cuts; green bars). Wounded leaf tissues (or equivalent unwounded controls) were sampled at 0.5 h and 1 h post-wounding. Expression was normalized relative to the reference genes *OsG3PDH* and *Ubiquitin 10* using the $2^{-\Delta\Delta Ct}$ method. Data represent the mean ±SE from three independent biological replicates, each with three technical replicates. Different letters above bars indicate statistically significant differences within each panel based on ANOVA followed by Fisher's LSD test ($P<0.05$). (H) Hierarchical clustering analysis (heatmap) of the relative expression patterns of JA biosynthesis genes (*OsAOC*, *OsOPR7*, *OsAOS1*, *OsAOS2*, and *OsJAR1*), JA signalling repressors (*OsJAZ8*, *OsJAZ9*, *OsJAZ10*, *OsJAZ11*, and *OsJAZ13*), and SA-responsive marker genes (*OsSGT1* and *OsWRKY45*) across all treatments and time points described above. Rows represent experimental conditions (clustered based on expression profile similarity), and columns represent genes (clustered based on co-expression patterns). Colour intensity corresponds to the $\log_2$-transformed fold change (as indicated by the scale bar), with red indicating up-regulation and blue indicating down-regulation. Data used for the heatmap correspond to the mean values from the RT-qPCR experiments.

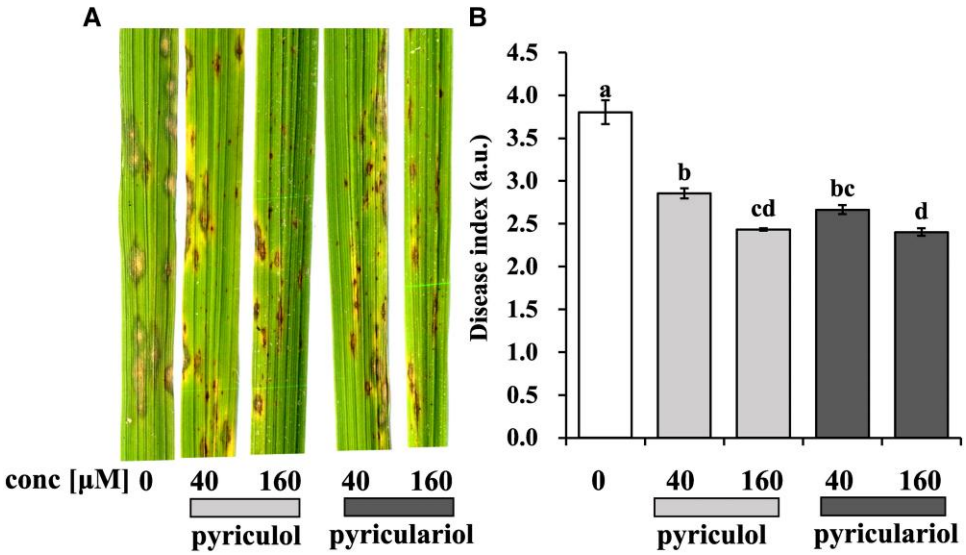

Fig. 5. Pyriculol and pyriculariol treatment reduces rice blast severity on the susceptible cultivar Nihonmasari. (A) Disease phenotypes on Nihonmasari leaves at 6 days post-inoculation (dpi) with *M. oryzae* Gy11 (5×10^4 spores ml^{-1}). Leaves were treated with pyriculol (Py) or pyriculariol (Pyl) at the indicated concentrations (40 µM and 160 µM), or with solvent control (0 µM; 1% methanol). (B) Disease Index (DI) quantifying symptom severity shown in (A). Lower DI values indicate reduced disease severity. Bars represent the mean ±SE (n=3 biological replicates). Statistical significance between treatments was determined by ANOVA followed by LSD test (P<0.05), denoted by different letters.

Overall, the mitigation of symptoms after pyriculol treatment (Fig. 5) is correlated with impaired hyphal spread, a stimulated host cell death, and a promoted oxidative burst in the attacked cell, but also in the adjacent cells.

Pyriculol and pyriculariol amplify the pathogen response of defence genes

To understand how pyriculol and pyriculariol alter the resistance of rice to *M. oryzae* (Fig. 5), we assessed a selected panel of defence genes.

The pathogenesis-related protein OsPR1a represents the acidic PR proteins, while OsPR1b is an important alkaline PR protein (Mitsuhara *et al.*, 2008). The transcript level of the corresponding/coding genes for both proteins were clearly induced, by ~30-fold, in response to infection (Fig. 7A, B). Pyriculol alone caused only a minor increase and amplified the response to *M. oryzae* in a multiplicative manner (not the logarithmic scale). In contrast, pyriculariol induced a substantial increase of both transcripts that almost reached the induction observed after infection. Interestingly, a combination of pyriculariol and fungal infection was not fully multiplicative; the induction was only slightly higher than for infection alone, indicating that both factors act through shared events. The pattern for *OsPR10a/PBZ1* encoding an RNase (Rakwal *et al.*, 2001) was comparable, with the exception that here pyriculariol only evoked a minor response, not different from pyriculol (Fig. 7C). As downstream events, we also probed transcripts for *OsCPS2* (Fig. 7D) and *OsCPS4* (Fig. 7E), involved in the biosynthesis of momilactone, an important rice phytoalexin (Lu *et al.*, 2018). Here, we observed a clear and strong synergy for *OsCPS2*, because pyriculol and pyriculariol alone were not inducive, but almost quadrupled the response to infection. Instead, for *OsCPS4*, the pattern resembled that for the *PR* genes, with a mild induction for pyriculol alone acting multiplicatively with infection, and a substantial induction for pyriculariol alone that increased the response to induction, but only partially, as if it were limited by some sort of saturation.

Discussion

The aim of the current study was to understand potential functions of pyriculol for the pathogenesis of *M. oryzae*. In our strategy, we compared the cellular and molecular response of hosts differing with respect to their susceptibility to this pathogen and confronted them with modified strains of *M. oryzae* differing with respect to pyriculol accumulation. Motivated by the structural similarity between pyriculol and SA, we monitored the responses to exogenous SA in parallel. We found that the host responses varied significantly depending on the ability of the respective strain to produce pyriculol. However, surprisingly, the lack of pyriculol did not impair the infection process, consistent with our previous findings where mutants deleted for the biosynthetic genes *MoPKS19* or *MoC19OXR1* remained fully pathogenic despite their inability to induce lesions *in vitro* (Jacob *et al.*, 2017). This confirms the paradox that the pathogen expends energy on a secondary metabolite that is seemingly dispensable for virulence, while, on the other hand, pyriculol enhanced oxidative burst and the expression of defence genes triggered by the pathogen. These data

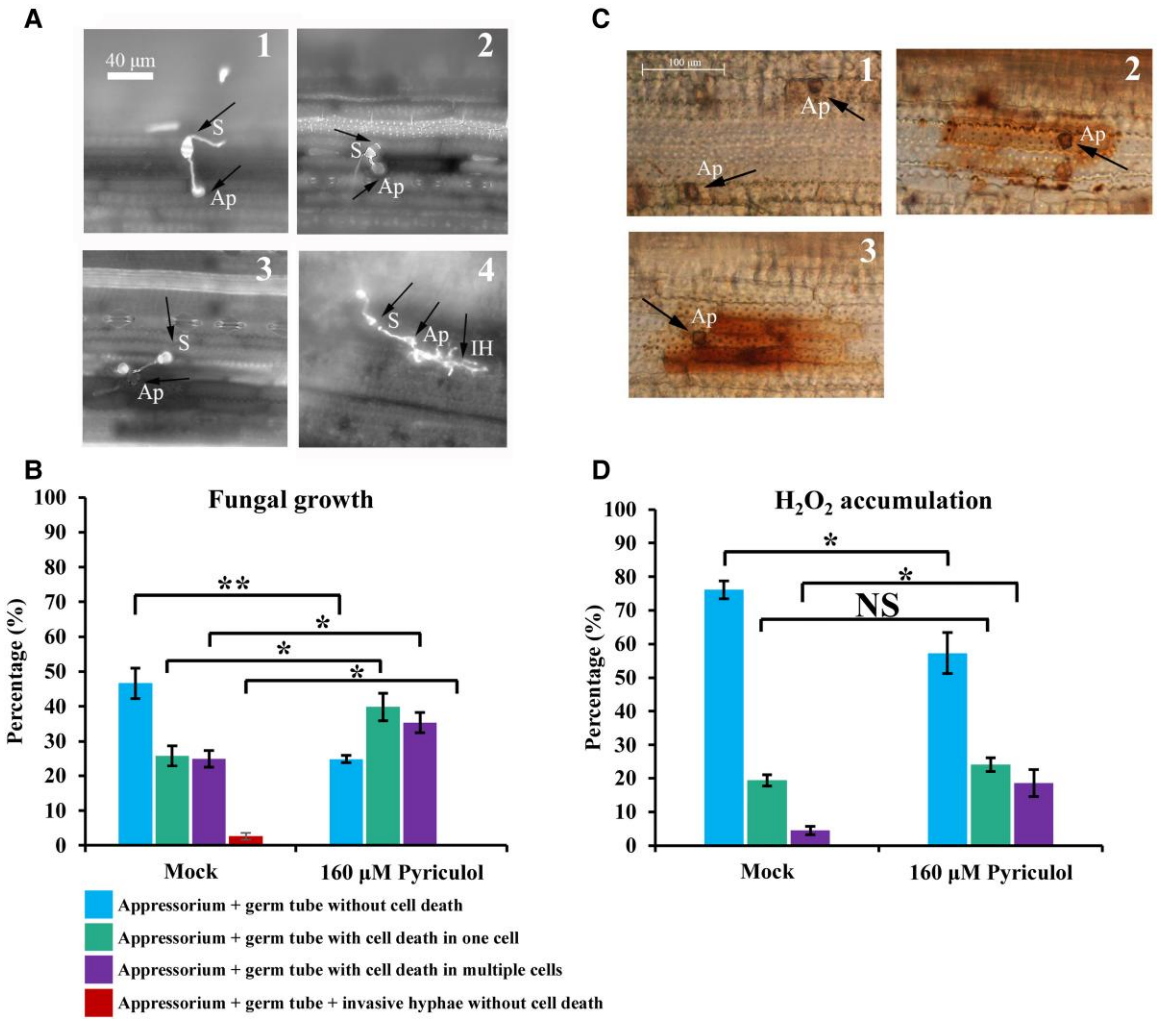

Fig. 6. Pyriculol and pyriculariol treatments modulate *M. oryzae* infection progression and associated host oxidative burst at the cellular level in the susceptible rice cv Nihonmasari. (A) Representative bright-field microscopy images (×20 magnification) illustrating categories of fungal infection stages on *O. sativa* cv Nihonmasari leaves. Plants were inoculated with *M. oryzae* Gy11 (5×10^4 spores ml^{-1}) and treated with pyriculol (160 µM), pyriculariol (160 µM), or solvent control (0 µM; 1% methanol). Categories shown are: (1) appressorium+germ tube, no host cell oxidative burst; (2) appressorium+germ tube, oxidative burst in the initially infected cell; (3) appressorium+germ tube, oxidative burst in surrounding cells; and (4) successful colonization with invasive hyphae, associated oxidative burst. (B) Quantification of the relative frequency of the fungal growth/host response categories depicted in (A). Data represent the mean percentage (±SE) from three biological replicates, with 100 infection sites assessed per replicate. Asterisks indicate significant differences compared with the solvent control (0 µM) as determined by Student's *t*-test ($P<0.05$, $^*P<0.01$). (C) Representative images of 3,3'-diaminobenzidine (DAB) staining visualizing H_2O_2 accumulation (brown precipitate) associated with the different infection categories described in (A). (D) Quantification of the frequency of infection sites exhibiting distinct H_2O_2 accumulation patterns (corresponding to the categories) based on DAB staining. Data presentation and replication are as in (B). Asterisks indicate significant differences compared with the solvent control (0 µM) determined by Student's *t*-test ($P<0.05$); NS, not significant.

stimulate some questions that will be discussed below. How does pyriculol integrate into the conceptual framework for plant–pathogen interaction? What is the mechanistic basis behind the different resistance levels of the different rice varieties? Is pyriculol hijacking SA signalling?

If pyriculol is not an effector, what is it?

Pyriculol was originally discovered due to its ability to induce necrotic lesions in rice that resembled those seen upon infection with *M. oryzae*, in those days known under the name *Pyricularia oryzae* (Iwasaki *et al.*, 1969). It is straightforward, therefore, to assign to pyriculol a role as a virulence factor. This role might be either that of an effector, silencing basal immunity, or that of a phytotoxin, killing the host cell, such that the intruder can scavenge its remains following a necrotrophic growth strategy. To address this, different strains were engineered that accumulated either more or less pyriculol compared with the wild-type strain (Jacob *et al.*, 2017). Using the *indica* dwarf genotype Co39, symptom expression was found to be unchanged no matter how much pyriculol was produced by the respective strain. However, since these data were limited to

one host genotype and the readout was checked only qualitatively without addressing fungal development, we wondered whether a more detailed look might reveal so far overlooked differences between the strains. The strains in which pyriculol biosynthetic enzymes were overexpressed showed the same symptom scores as the non-transformed wild-type strain. Crucially, the ΔMoPKS19 mutant (with abolished pyriculol/pyriculariol production) and the ΔMoC19OXR1 mutant (which specifically accumulates biologically inactive dihydro derivatives instead of active pyriculol) maintained virulence levels equivalent to the wild type (Jacob *et al.*, 2017). Although we could not quantify pyriculol concentration *in planta*, probably due to rapid detoxification or sequestration by the host preventing toxin accumulation to detectable levels (Jacob *et al.*, 2017), these genetic data conclusively confirm that pyriculol production is not essential for pathogenicity. In contrast, the strains ΔMoC19tf1 and ΔMoC19tf2, where two negative regulators of biosynthesis were knocked down, did not display the expected enhancement of symptoms, but rather a clear mitigation (Fig. 1B). This reduced pathogenicity, despite the up-regulation of pyriculol biosynthesis, implies distinct physiological roles for these transcription factors (Jacob *et al.*, 2017). Consistent with the observed phenotype, we postulate that MoC19tf1 and MoC19tf2 are likely to exert a dual regulatory function: acting as negative regulators of pyriculol but serving as positive regulators for other unidentified virulence pathways. Consequently, in the deletion mutants, the down-regulation of these critical virulence factors over-rides the effect of increased pyriculol production. We confirmed, however, that pyriculol alone can induce lesions that look fairly similar to those induced by the fungus (compare Fig. 2A and Fig. 1A).

The crucial criterion to define a compound as an effector is that it can silence the expression of defence genes. If pyriculol acted as an effector, the strain with the mildest symptom expression should be the strain which most effectively eliminates the response of defence genes. However, we observed that this strain strongly enhanced the response of all tested defence genes compared with the level seen for the wild type. Thus, the effect of pyriculol is just the opposite of that which would be expected from an effector.

We conclude that (i) pyriculol is not an effector, (ii) pyriculol alone can induce necrotic lesions, but (ii) pyriculol is not a necessary factor for successful infection, and (iv) the formation of lesions rather is inversely correlated with the activation of defence genes.

The lesions induced by pyriculol were originally interpreted as manifestation of a HR (Iwasaki *et al.*, 1969) as it is observed upon infection with a strain carrying an avirulence gene (Wang *et al.*, 2017). However, it might be misleading to consider the two phenomena as equal. The presence of an avirulence gene leads to strong induction of defence genes, such as the JA synthesis gene *OsAOS2*, the JA response gene *OsJAZ9*, the pathogenesis-related *OsPR1b*, or the phytoalexin biosynthesis gene *OsCPS2* (Ma *et al.*, 2022). In the current study, the response of some of these genes was clearly reversed—transcript levels were suppressed, rather than being induced (Figs 3, 4). Thus, it would be misleading to interpret the lesions induced by pyriculol as a HR.

Regarding the nature of these lesions, it is important to address the morphological discrepancy between the symptoms induced by pyriculol and SA (Fig. 2). While the pyriculol-induced lesions feature a more prominent blackish necrotic ring, this probably reflects the deposition of condensed phenolic compounds, such as tannins, prior to the onset of necrosis. Since both pyriculol and SA trigger identical molecular signatures—specifically the suppression of wounding response genes (*OsAOS2* and *OsJAZ2*) (Fig. 3) and the additive activation of SA-responsive genes (*OsSGT1* and *OsWRKY45*) (Fig. 4)—we propose that the effect of pyriculol is mediated through the SA pathway. In this model, direct SA application may simply bypass the accumulation of pigmented intermediates to initiate necrosis more rapidly. Consequently, these subtle differences in pigment formation do not negate the primary functional equivalence established at the molecular level. It should also be noted that the concentrations of exogenous pyriculol used here are higher than those typically produced by the colonizing fungus. This dosage was technically necessary to overcome rapid host detoxification and reveal the mode of action of the molecule *in vitro*; thus, the observed necrosis might represent a consequence of high local accumulation rather than being the primary physiological function during infection.

However, our data suggest that the actual function of pyriculol *in planta* is not that of a phytotoxin, but rather a signalling modulator. Still, although we can rule out the classic roles—effector or phytotoxin—the actual function of pyriculol remains unclear. We wondered whether the real target of pyriculol might be competing fungi, rather than the plant host. While seldom addressed, allelopathic interactions between fungi are of tremendous ecological importance (Osivand *et al.*, 2018). However, the very high concentrations of pyriculol required to elicit even marginal effects on germination (Supplementary Fig. S4) argue against a strong allelopathic potential of this compound. Nevertheless, as *Magnaporthe* itself synthesizes pyriculol, some level of self-tolerance is expected, and its ecological role—if any—might instead be to target other microorganisms or plant species rather than affecting the germination of the producer itself. We therefore ventured to gain some insight into the function of pyriculol by comparing the responses of a pair of host genotypes that differ with respect to their susceptibility to *M. oryzae*.

Lesion formation correlates with low expression of *OsPBZ1*

When we compared expression of a set of representative defence genes with lesion formation in the moderately resistant Co39 versus the susceptible Maratelli, we observed the same level of *OsCPS4*, while the two PR genes were induced

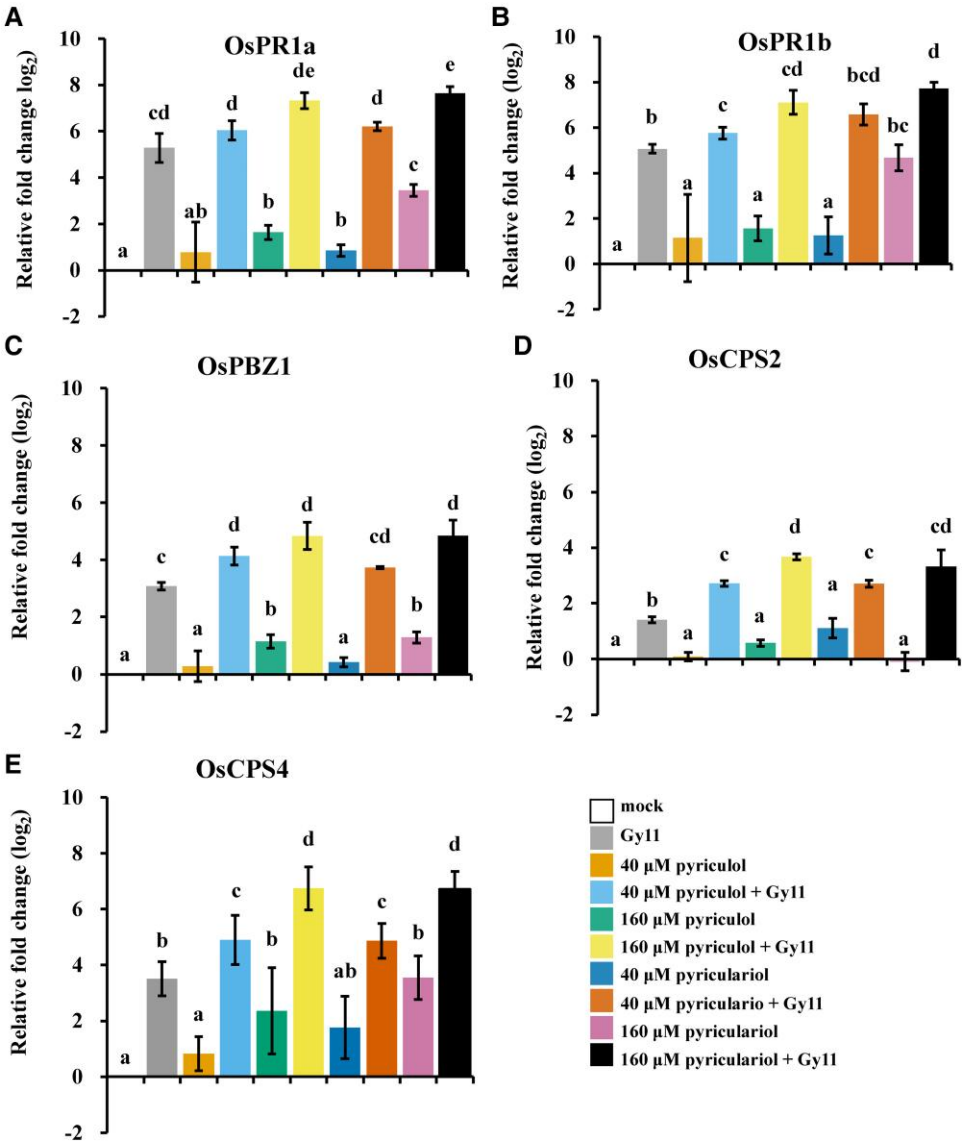

Fig. 7. Pyriculol and pyriculariol treatments differentially modulate the expression of defence-related and phytoalexin biosynthesis genes in rice. Relative expression levels (log_2 fold change) of (A) *OsPR1a*, (B) *OsPR1b*, (C) *OsPBZ1*, (D) *OsCPS2*, and (E) *OsCPS4* were quantified by RT-qPCR in the fourth leaf blades of *O. sativa* cv Nihonmasari at 2 days post-inoculation (dpi). Plants were subjected to treatments as indicated: mock control; inoculation with *M. oryzae* strain Gy11 (5×10^4 spores ml^{-1}); treatment with 40 μM or 160 μM pyriculol; treatment with 40 μM or 160 μM pyriculariol; or combined chemical and Gy11 inoculation. Gene expression was quantified using the $2^{-\Delta\Delta Ct}$ method, normalized against the geometric mean of *OsG3PDH* and *Ubiquitin 10* reference genes, and expressed relative to the mock control. Data represent means ±SE from three independent biological replicates, each assessed with three technical replicates. Different letters above the bars indicate statistically significant differences among treatments within each gene panel ($P<0.05$, Fisher's LSD test following one-way ANOVA).

much more strongly in the susceptible than in the resistant genotype (Fig. 1C–F). For the acidic OsPR1a, the weaker induction in Co39 still led to the same steady-state levels for this transcript as in the apparently more responsive Maratelli, because the ground levels in Co39 were already elevated. Also, the ground levels of OsPBZ1 were significantly higher in Co39, but here infection induced twice as much of the transcript in Maratelli than in Co39. For the interpretation of the transcript levels, it is important to consider that they were measured at day 2 after inoculation, which means that it is safe to assume that a steady state has been reached, such that induced transcript levels for a given gene are likely to stem from increased demand of the respective protein.

The correlation of susceptibility with a stronger accumulation of *OsPBZ1* transcripts in Maratelli leads to the question of the physiological function of this gene. Its discovery is linked with probenazole, used as a fungicide to control rice blast (Watanabe *et al.*, 1977). However, this compound was later

found to act as an inducer of transcripts for a pathogenesis-related protein, OsPBZ1 (Midoh and Iwata, 1996), which turned out to be an RNase inducing programmed cell death linked with the accumulation of SA (Iwai *et al.*, 2007). Thus, a straightforward hypothesis for the inverse relationship between lesion formation and expression of this gene would be to assume that the lesions derive from SA-dependent programmed cell death triggered by OsPBZ1.

This hypothesis is further substantiated by the spatial dynamics of reactive oxygen species (ROS). While bulk measurements of H_2O_2 concentration often fail to capture localized signalling events due to dilution effects from healthy tissue, our histological quantification of H_2O_2 spatial patterns provides a more biologically relevant insight (Fig. 6). We observed that pyriculol significantly increased the frequency of infection sites, exhibiting a systemic spread of H_2O_2 accumulation (extending to adjacent cells) and concomitant host cell death. This shift from a localized to a systemic oxidative burst represents a hallmark of an effective defence mobilization (Fig. 6C), confirming that pyriculol acts to lower the threshold for triggering defence responses rather than suppressing them.

These considerations lead to alternative viewpoints on the role of pyriculol in the hormonal crosstalk between SA and JAs.

Is pyriculol promoting infection by uncoupling systemic and local jasmonic acid responses?

As expected from the structural similarity, pyriculol could mimic SA almost perfectly: the induction of lesions, the mitigation of early JA synthesis and response genes upon wounding, and the similar additivity with respect to the induction of *OsSGT1* and *OsWRKY45* used as reporters for the activity of SA responses demonstrate a high degree of functional equivalence. Actually, we could identify only one trait where the two compounds differed—the wounding response for the final gene of the JA pathway, *OsJAR1*, encoding the ligase converting the inactive JA to the active isoleucine conjugate is silenced by pyriculol, but not by SA (Fig. 3E), leading to the question of whether pyriculol disrupts the interaction between JAs and SA.

The interaction of both hormones is a crucial factor for the ensuing defence strategy. While JAs are central for the wounding response and the defence against necrotrophic pathogens (where programmed cell death is not meaningful), SA is associated with the defence against biotrophic pathogens (where programmed cell death represents an efficient strategy). Since this antagonism has been reported for a large number of taxa, it is thought to have arisen early in evolution (Thaler *et al.*, 2012). The decision between JA and SA is nothing less than a decision for the best strategy—either cellular defence (the attacked cell combats the intruder, for instance by phytoalexins) or systemic defence (the attacked cell commits suicide to block the spread of the intruder). It is not surprising that this decision is checked and reinforced on several tiers of the response. For instance, the master regulator of SA-induced gene expression, NONEXPRESSER OF PR GENES1 (NPR1), can bind and block MYC2, the master regulator of JA-induced gene expression (Nomoto *et al.*, 2021). Conversely, stimulation of MYC2 activity by JAs will suppress SA responses (Thaler *et al.*, 2012).

Disruption of the functional link between JAs and SA would provide a lever for pathogens to hijack plant defence. In fact, the suppression of hypersensitive cell death by the bacterial effector coronatine, a highly potent mimic of bioactive JAs in the interaction of *P. syringae* with *A. thaliana*, represents a classic case of this strategy (Brooks *et al.*, 2005).

Pyriculol seems a perfect mimic of SA with respect to silencing wound induction of genes of early JA synthesis and response. Despite the subtle morphological distinctions in necrotic symptoms mentioned above, the molecular signalling remains consistent. There is only one, but significant, exception: OsJAR1, the conjugase converting the inactive precursor JA into the active JA-Ile conjugate. The wound induction of this gene is suppressed by SA, but not by pyriculol. What are the consequences? Why should a difference in the activity of the final gene in the pathway play any role if the preceding steps are all silenced anyway? The precursor, JA, harbours an alternative option from being ligated into JA-Ile—it can also be methylated and travel far in this volatile form. Upon arrival in the target cell, it is again demethylated and then available for conversion into JA-Ile (Seo *et al.*, 2001). Thus, SA would prevent the accumulation of bioactive JA-Ile whether the precursor JA has been synthesized locally or has been imported as MeJA and then released by demethylation. In contrast, pyriculol would intercept any active JA from local synthesis, but would allow conversion of JA generated elsewhere and imported as MeJA. In other words, pyriculol would interfere only with local, but be permissive to systemic, JA effects.

In our previous work (Ma *et al.*, 2022), we had compared the response to *M. oryzae* between a *japonica* wild type, Nihonmasari, and two mutants, *cpm2* and *hebiba*, where the function of AOC, the enzyme generating the precursor OPDA, had been disrupted. In both mutants, the pathogen was more efficient in advancing development during primary invasion of a host cell and also during the progression to neighbouring cells, incompatible interactions, which was linked with a larger extension of necrosis. A similar phenotype was observed in a Tos17 mutant, where OsJAR1, the final ligase, had been disrupted (Riemann *et al.*, 2013). These findings support a scenario where JA-Ile acts as a negative regulator of programmed cell death, mainly during early fungal spread. This negative regulation would support suppressed synthesis or signalling of SA during early spread. At a later stage, when the pathogen moves to a necrotrophic phase, it would be advantageous to relieve this antagonistic interaction. In contrast to SA, pyriculol would allow systemic MeJA to be converted into JA-Ile. This JA-Ile would then act independently of SA (which had been suppressed previously). The apparent discrepant findings based on exogenously applied SA or pyriculol fail to mimic

the decisive temporal pattern of a natural infection, where JA-Ile first acts together with SA, but later, by being formed from systemic MeJA that had been imported from neighbouring cells, acts in the absence of SA and then evokes necrosis that is actually supporting necrotrophic fungal development.

Thus, the subtle effect of pyriculol might be the temporal uncoupling of SA and JAs. To pinpoint this would require a different type of experimentation, where the three signals (JAs, SA, and pyriculol) are administered in defined and reversed temporal order to test whether this temporal signature would lead to qualitatively different outcomes.

Supplementary data

The following supplementary data are available at *JXB* online.

Fig. S1. Representative infection symptoms on rice varieties Co39 and Maratelli following inoculation with seven *M. oryzae* mutants exhibiting varying levels of pyriculol production.

Fig. S2. Expression stability analysis of reference genes *OsGAPDH* and *OsU10* across experimental conditions.

Fig. S3. RT-qPCR expression analysis of defence marker genes *OsPR1a*, *OsPBZ1*, and *OsCPS4* in Co39 and Maratelli rice cultivars at 48 h post-inoculation with different *M. oryzae* strains.

Fig. S4. Quantitative analysis of *M. oryzae* conidial germination rates in response to increasing concentrations of exogenous pyriculol and pyriculariol.

Table S1. Details and descriptions of the *Magnaporthe oryzae* 70-15 wild-type and mutant strains used in this study, including their specific pyriculol and pyriculariol production levels *in vitro*.

Table S2. Primers used for RT-PCR.

Acknowledgements

JM thanks the China Scholarship Council and Karlsruhe House of Young Scientists for supporting his PhD programme.

Author contributions

JBM and MR: conceptualization; JM: investigation; JM and PN: formal analysis and writing—original draft; PN, JBM, and SJ: writing—review & editing; SJ: resources; PN: supervision and funding acquisition.

Conflict of interest

The authors state that no conflict of interest exists regarding this publication.

Data availability

The primary data supporting this study were not made publicly available at the time of publication. Data will be made available upon request to the corresponding author, Peter Nick.

References

Akagi A, Fukushima S, Okada K, Jiang CJ, Yoshida R, Nakayama A, Shimono M, Sugano S, Yamane H, Takatsuji H. 2014. WRKY45-dependent priming of diterpenoid phytoalexin biosynthesis in rice and the role of cytokinin in triggering the reaction. Plant Molecular Biology **86**, 171–183.

Andersen CL, Jensen JL, Ørntoft TF. 2004. Normalization of real-time quantitative reverse transcription–PCR data: a model-based variance estimation approach to identify genes suited for normalization, applied to bladder and colon cancer data sets. Cancer Research **64**, 5245–5250.

Brooks D, Bender C, Kunkel B. 2005. The *Pseudomonas syringae* phytotoxin coronatine promotes virulence by overcoming salicylic acid-dependent defences in *Arabidopsis thaliana*. Molecular Plant Pathology **6**, 629–639.

Chanclud E, Kisiala A, Emery NR, Chalvon V, Ducasse A, Romiti-Michel C, Gravot A, Kroj T, Morel JB. 2016. Cytokinin production by the rice blast fungus is a pivotal requirement for full virulence. PLoS Pathogens **12**, e1005457.

Djamei A, Schipper K, Rabe F, *et al.* 2011. Metabolic priming by a secreted fungal effector. Nature **478**, 395–398.

Duan L, Liu H, Li X, Xiao J, Wang S. 2014. Multiple phytohormones and phytoalexins are involved in disease resistance to *Magnaporthe oryzae* invaded from roots in rice. Physiologia Plantarum **152**, 486–500.

Friesen TL, Faris JD, Solomon PS, Oliver RP. 2008. Host-specific toxins: effectors of necrotrophic pathogenicity. Cellular Microbiology **10**, 1421–1428.

Iwai T, Seo S, Mitsuhara I, Ohashi Y. 2007. Probenazole-induced accumulation of salicylic acid confers resistance to *Magnaporthe grisea* in adult rice plants. Plant & Cell Physiology **48**, 915–924.

Iwasaki S, Nozoe S, Okuda S, Sato Z, Kozaka T. 1969. Isolation and structural elucidation of a phytotoxic substance produced by *Pyricularia oryzae* Cavara. Tetrahedron Letters **10**, 3977–3980.

Jacob S, Grotsch T, Foster AJ, Schuffler A, Rieger PH, Sandjo LP, Liermann JC, Opatz T, Thines E. 2017. Unravelling the biosynthesis of pyriculol in the rice blast fungus *Magnaporthe oryzae*. Microbiology **163**, 541–553.

Kato-Noguchi H. 2023. Defensive molecules momilactones a and b: function, biosynthesis, induction and occurrence. Toxins **15**, 241.

Kono Y, Sekido S, Yamaguchi I, Kondo H, Suzuki Y, Neto GC, Sakurai A, Yaegashi H. 1991. Structures of two novel pyriculol-related compounds and identification of naturally produced epipyriculol from *Pyricularia oryzae*. Agricultural and Biological Chemistry **55**, 2785–2791.

Liu W, Liu J, Ning Y, Ding B, Wang X, Wang Z, Wang G. 2013. Recent progress in understanding PAMP- and effector-triggered immunity against the rice blast fungus *Magnaporthe oryzae*. Molecular Plant **6**, 605–620.

Livak KJ, Schmittgen TD. 2001. Analysis of relative gene expression data using real-time quantitative PCR and the $2^{-\Delta\Delta CT}$ method. Methods **25**, 402–408.

Lokeshwari TS, Suryanarayanan S. 1992. Induction of 'green islands'in rice leaves by EDTA and some toxins of *Pyricularia oryzae* Cav. Journal of Plant Diseases and Protection **99**, 286–292.

Lu X, Zhang J, Brown B, *et al.* 2018. Inferring roles in defense from metabolic allocation of rice diterpenoids. The Plant Cell **30**, 1119–1131.

Ma J, Morel JB, Riemann M, Nick P. 2022. Jasmonic acid contributes to rice resistance against *Magnaporthe oryzae*. BMC Plant Biology **22**, 601.

Midoh N, Iwata M. 1996. Cloning and characterization of a probenazole-inducible gene for an intracellular pathogenesis-related protein in rice. Plant & Cell Physiology **37**, 9–18.

Mitsuhara I, Iwai T, Seo S, Yanagawa Y, Kawahigasi H, Hirose S, Ohkawa Y, Ohashi Y. 2008. Characteristic expression of twelve rice PR1 family genes in response to pathogen infection, wounding, and defense-related signal compounds (121/180). Molecular Genetics and Genomics **279**, 415–427.

Nomoto M, Skelly MJ, Itaya T, *et al.* 2021. Suppression of MYC transcription activators by the immune cofactor NPR1 fine-tunes plant immune responses. Cell Reports **37**, 110125.

Osivand A, Araya H, Appiah KS, Mardani H, Ishizaki T, Fujii Y. 2018. Allelopathy of wild mushrooms–an important factor for assessing forest ecosystems in Japan. Forests **9**, 773.

Rakwal R, Agrawal GK, Yonekura M. 2001. Light-dependent induction of OsPR10 in rice (*Oryza sativa* L.) seedlings by the global stress signaling

molecule jasmonic acid and protein phosphatase 2A inhibitors. Plant Science **161**, 469–479.

Riemann M, Haga K, Shimizu T, *et al.* 2013. Identification of rice allene oxide cyclase mutants and the function of jasmonate for defence against *Magnaporthe oryzae*. The Plant Journal **74**, 226–238.

Seo HS, Song JT, Cheong JJ, Lee YH, Lee YW, Hwang I, Lee JS, Choi YD. 2001. Jasmonic acid carboxyl methyltransferase: a key enzyme for jasmonate-regulated plant responses. Proceedings of the National Academy of Sciences, USA **98**, 4788–4793.

Shimizu T, Miyamoto K, Miyamoto K, Minami E, Nishizawa Y, Iino M, Nojiri H, Yamane H, Okada K. 2013. OsJAR1 contributes mainly to biosynthesis of the stress-induced jasmonoyl-isoleucine involved in defense responses in rice. Bioscience, Biotechnology, and Biochemistry **77**, 1556–1564.

Silverman P, Seskar M, Kanter D, Schweizer P, Metraux J-P, Raskin I. 1995. Salicylic acid in rice (biosynthesis, conjugation, and possible role). Plant Physiology **108**, 633–639.

Suzuki M, Sugiyama T, Watanabe M, Yamashita K. 1986. Synthesis of optically active pyriculol, a phytotoxic metabolite produced by *Pyricularia oryzae* Cavara. Agricultural and Biological Chemistry **50**, 2159–2160.

Tamaoki D, Seo S, Yamada S, Kano A, Miyamoto A, Shishido H, Miyoshi S, Taniguchi S, Akimitsu K, Gomi K. 2013. Jasmonic acid and salicylic acid activate a common defense system in rice. Plant Signaling & Behavior **8**, e24260.

Thaler JS, Humphrey PT, Whiteman NK. 2012. Evolution of jasmonate and salicylate signal crosstalk. Trends in Plant Science **17**, 260–270.

Uji Y, Taniguchi S, Tamaoki D, Shishido H, Akimitsu K, Gomi K. 2016. Overexpression of OsMYC2 results in the up-regulation of early JA-responsive genes and bacterial blight resistance in rice. Plant & Cell Physiology **57**, 1814–1827.

Umemura K, Satou J, Iwata M, Uozumi N, Koga J, Kawano T, Koshiba T, Anzai H, Mitomi M. 2009. Contribution of salicylic acid glucosyltransferase, OsSGT1, to chemically induced disease resistance in rice plants. The Plant Journal **57**, 463–472.

Vandesompele J, De Preter K, Pattyn F, Poppe B, Van Roy N, De Paepe A, Speleman F. 2002. Accurate normalization of real-time quantitative RT–PCR data by geometric averaging of multiple internal control genes. Genome Biology **3**, Research0034.

Wang B-H, Ebbole DJ, Wang Z-H. 2017. The arms race between *Magnaporthe oryzae* and rice: diversity and interaction of Avr and R genes. Journal of Integrative Agriculture **16**, 2746–2760.

Wasternack C, Feussner I. 2018. The oxylipin pathways: biochemistry and function. Annual Review of Plant Biology **69**, 363–386.

Watanabe T, Igarashi H, Matsumoto K, Seki S, Mase S, Sekizawa Y. 1977. Characteristics of probenazole (Oryzemate) for the control of rice blast. Journal of Pesticide Science **2**, 291–296.

Yan X, Tang B, Ryder LS, *et al.* 2023. The transcriptional landscape of plant infection by the rice blast fungus *Magnaporthe oryzae* reveals distinct families of temporally co-regulated and structurally conserved effectors. The Plant Cell **35**, 1360–1385.

Yin C, Park JJ, Gang DR, Hulbert SH. 2014. Characterization of a tryptophan 2-monooxygenase gene from *Puccinia graminis* f. sp. *tritici* involved in auxin biosynthesis and rust pathogenicity. Molecular Plant-Microbe Interactions **27**, 227–235.

Zhu X, Zhao Y, Shi CM, *et al.* 2024. Antagonistic control of rice immunity against distinct pathogens by the two transcription modules via salicylic acid and jasmonic acid pathways. Developmental Cell **59**, 1609–1622.